

Embolic Doppler Ultrasound Signal Detection Using Discrete Wavelet Transform

Nizamettin Aydin, *Member, IEEE*, Farokh Marvasti, *Senior Member, IEEE*, and Hugh S. Markus

Abstract—Asymptomatic circulating emboli can be detected by Doppler ultrasound. Embolic Doppler ultrasound signals are short duration transient like signals. The wavelet transform is an ideal method for analysis and detection of such signals by optimizing time-frequency resolution. We propose a detection system based on the discrete wavelet transform (DWT) and study some parameters, which might be useful for describing embolic signals (ES). We used a fast DWT algorithm based on the Daubechies eighth-order wavelet filters with eight scales. In order to evaluate feasibility of the DWT of ES, two independent data sets, each comprising of short segments containing an ES ($N = 100$), artifact ($N = 100$) or Doppler speckle (DS) ($N = 100$), were used. After applying the DWT to the data, several parameters were evaluated. The threshold values used for both data sets were optimized using the first data set. While the DWT coefficients resulting from artifacts dominantly appear at the higher scales (five, six, seven, and eight), the DWT coefficients at the lower scales (one, two, three, and four) are mainly dominated by ES and DS. The DWT is able to filter out most of the artifacts inherently during the transform process. For the first data set, 98 out of 100 ES were detected as ES. For the second data set, 95 out of 100 ES were detected as ES when the same threshold values were used. The algorithm was also tested with a third data set comprising 202 normal ES; 198 signals were detected as ES.

Index Terms—Cerebral emboli, detection, discrete wavelet transform (DWT), fuzzy logic, ultrasound, wavelet.

I. INTRODUCTION

ASYMPTOMATIC circulating cerebral emboli can be detected by transcranial Doppler ultrasound [1]. In certain conditions, such as carotid artery stenosis, asymptomatic embolic signals (ES) appear to be markers of increased stroke risk and may be useful in patient management [2]. A major problem with clinical implementation of the technique is the lack of a reliable automated system of ES detection. Recordings in patients may need to be one or more hours in duration and analyzing the spectra visually is time consuming and subject to observer fatigue and error. While interobserver reproducibility studies have demonstrated that there is an overall high level of agreement in identifying ES, this is poorest for ES of low relative intensity [3]. Any processing method, which improves the ratio of the ES to the background blood signal (EBR), will improve the performance of an automated system.

Manuscript received June 19, 2002; revised March 28, 2003. This work was supported by the British Heart Foundation under Project Grant PG99064.

N. Aydin is with the School of Engineering and Electronic, The University of Edinburgh, Edinburgh EH9 3JL, U.K. (e-mail: naydin@ee.ed.ac.uk).

F. Marvasti is with the Sharif University of Technology and Iran Telecommunications Research Center, Tehran, Iran.

H. S. Markus is with Clinical Neuroscience, St. George's Hospital Medical School, London SW17 0RE, U.K.

Digital Object Identifier 10.1109/TITB.2004.828882

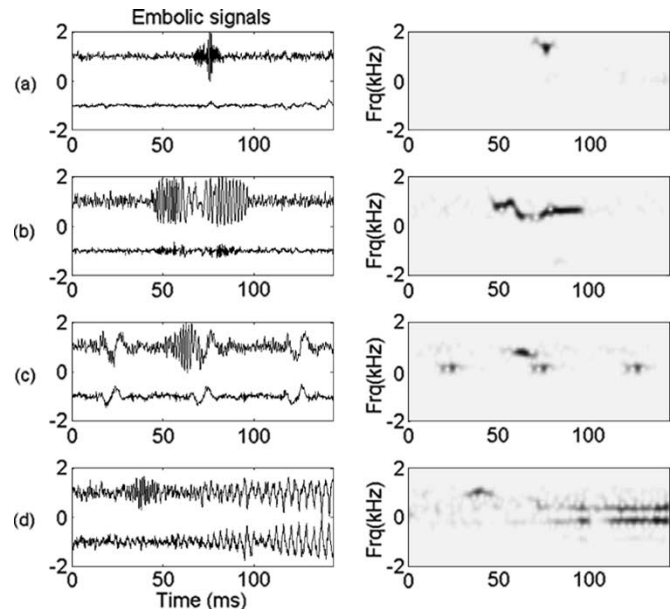


Fig. 1. Examples of normalized ES seen *in vivo* and corresponding TF distributions. For clarity, forward and reverse flow components are scaled by 1 and -1 , respectively.

Embolic Doppler ultrasound signals reflected by emboli, which are much bigger than red blood cells, have some distinctive characteristics when compared to high intensity signals from normal blood flow, which are termed as Doppler speckle (DS), and artifacts caused by tissue movement, probe tapping, speaking, etc. They appear as increasing and then decreasing in intensity for a short duration, usually less than 300 ms [4]. The bandwidth of ES is usually much less than that of DS. Therefore, they can be considered as narrow-band signals relative to DS [5]. They are also oscillating and finite signals like wavelets. On the other hand, DS are random fluctuations in the intensity of Doppler signals from blood flow and are band-limited signals as they are caused by many small scatterers (red blood cells) within the ultrasonic sample volume. DS does not have an associated characteristic click or chirping sound which is always associated with ES, and the distribution of high signal is more random rather than rising to a peak at a single frequency. Unlike artifacts, ES are unidirectional and usually contained within the flow spectrum [6]. The spectral content of an ES is also time dependent. Fig. 1 illustrates some examples of ES (forward and reverse flow components) seen *in vivo* and corresponding time-frequency (TF) representations. The ES in Fig. 1(a) is well defined. Detection of such ES is quite easy. The ES in Fig. 1(b) has a complex TF structure. ES corrupted by large artifacts are shown in Fig. 1(c) and (d).

An implication of this is that simple analysis and detection techniques are likely to fail.

A number of methods to detect cerebral emboli and to discriminate them from artifacts using Doppler ultrasound have been studied in the literature. These include discrimination of ES based on audio–visual characteristics [7], [8], spectral analysis [9], automated detection software [6], a trained neural network [10], a coincidence method [11], a TF processing based on spectrogram [12], [13], a frequency filtering method based on bandpass filters with a fixed bandwidth [14], a rule-based expert system [15], an off-line automated emboli detection based on the pseudo-Wigner power distribution [16], a TF analysis method based on the matching pursuit [17], [18], and use of power m-mode Doppler for tracking emboli [19]. A number of researchers have reported that the continuous wavelet transform (WT) performs better than the fast Fourier transform (FFT) for analysis and detection of ES [20]–[22]. The existence of fast algorithms to implement the discrete wavelet transform (DWT) also makes the investigation of the feasibility of ES detection systems based on the DWT worthwhile. Moreover, the DWT is ideal to suppress unwanted signals such as artifact, white noise, and DS [23]. In this study, we used the DWT to decompose an ES into different frequency bands and determined which features most accurately describe ES over the scales. We then investigated how to utilize these features in an on-line system.

II. DWT ANALYSIS OF DOPPLER SIGNALS

A. Wavelet Transform

For the TF analysis of a signal, a number of methods have been used. A desired property for any method is the availability of a fast algorithm allowing implementation in real time. This is exactly what made the Fourier transform so popular. With the advent of fast computers, the FFT has been extensively used for the TF analysis of signals in a wide range of fields. As an analogy to what the FFT does for the Fourier transform, an efficient method called the fast wavelet transform has been developed to implement the DWT using filters [24].

The WT of a continuous time signal $s(t)$ is defined as

$$W_s(a, b) = \frac{1}{\sqrt{a}} \int_{-\infty}^{+\infty} s(t) \psi \left(\frac{t-b}{a} \right) dt \quad (1)$$

where a is the scale, b is the translation, and $\psi_{a,b}$ is the mother wavelet. The WT in (1) is highly redundant and the parameters a and b are continuous. Application of the WT in practice is achieved using digital computers. Therefore, the WT is evaluated on a discrete grid on the time-scale plane corresponding to a discrete set of continuous basis function. A DWT yields a countable set of coefficients, which correspond to the points on a two-dimensional grid of discrete points in the time-scale domain [25]. The DWT of a signal is defined with respect to a mother wavelet and maps continuous finite energy signals to a two-dimensional grid of coefficients

$$W_s(m, n) = \frac{1}{\sqrt{a_0^m}} \int_{-\infty}^{+\infty} s(t) \psi \left(\frac{t - nb_0 a_0^m}{a_0^m} \right) dt \quad (2)$$

where m and n are discrete scale and translation steps. The scale a in the continuous WT case becomes $a = a_0^m$, and the translation b becomes $b = nb_0 a_0^m$ in the DWT. a_0 and b_0 are discrete scale and translation step sizes, respectively. When a discrete time finite energy signal with length N is considered, its DWT is a discrete inner product, which can be written as a circular convolution

$$W_s(m, n) = \frac{1}{\sqrt{a_0^m}} \sum_{k=0}^{N-1} s(k) \psi \left(\frac{k - nb_0 a_0^m}{a_0^m} \right) \quad (3)$$

where $\psi_{m,n}$ is the wavelet function. The DWT of a discrete signal yields a set of coefficients including all the detailed coefficients and the last approximation coefficient [26]. Under certain conditions [27], reconstructing a signal from its wavelet coefficients is also possible. The process is called the inverse discrete wavelet transform (IDWT) and involves interpolation and filtering.

B. DWT Description of DS, ES, and Artifacts

Prior to the study of DS, ES, and artifacts, it is instructive to investigate the DWT of Gaussian white noise (GWN) and compare it with the DWT of ES, DS, and artifacts. For this study, a complex GWN $n(k)$ of length 2048, was generated numerically. The DWT (eight scales) was applied to the signal. An eighth-order Daubechies wavelet was used for the analysis. The detailed coefficients were independently reconstructed and some simple statistics such as peak value and variance were calculated on the instantaneous power (IP) [28] of the reconstructed scales. The same processes were applied to a data set comprising the forward and reverse flow components of 100 ES, 100 DS, and 100 Doppler signals with artifacts, each of a standard 5-s duration. The sampling frequency was 7150 Hz. Average peak values and variances of IP for each scale of the forward and reverse flow components were calculated, and then the results were normalized to one for both flow directions separately. The average normalized peak values ($pemf/pemr$, $pspf/pspr$, $parf/parr$), and average normalized variances ($vemf/vemr$, $vspf/vspr$, $varf/varr$) of IP for each scales of forward–reverse flow components of ES, DS, and artifacts, respectively, as compared to the peak IP and variance for the GWN ($pgwn$ and $vgwn$, respectively) are illustrated in Fig. 2. The $pgwn$ halves and $vgwn$ quarters approximately with increasing scale. This is the expected pattern seen on the ES detection systems when there is no signal.

From Fig. 2(a) and (c), it is apparent that the ES concentrate on the Scales 2, 3, and 4, the DS concentrate on the Scales 1, 2, and 3, and the artifacts concentrate on the Scales 5 and 6. They do not follow the same pattern as the GWN for the forward flow signals. For the reverse flow signals, both the ES and DS display a similar pattern as the GWN [Fig. 2(b) and (d)], implying that both are mostly unidirectional. Large values of $pemr$ and $vemr$ in Scale 5 [Fig. 2(b) and (c)] are due to the existence of some artifacts. The reverse component of the artifact has almost the same characteristics as the forward components, confirming that most of the artifacts are bidirectional. Identifying and eventually suppressing these artifacts using the WT is quite straightforward. Although both are directional, ES differ from DS in certain aspects. They are much shorter in time, have higher amplitudes,

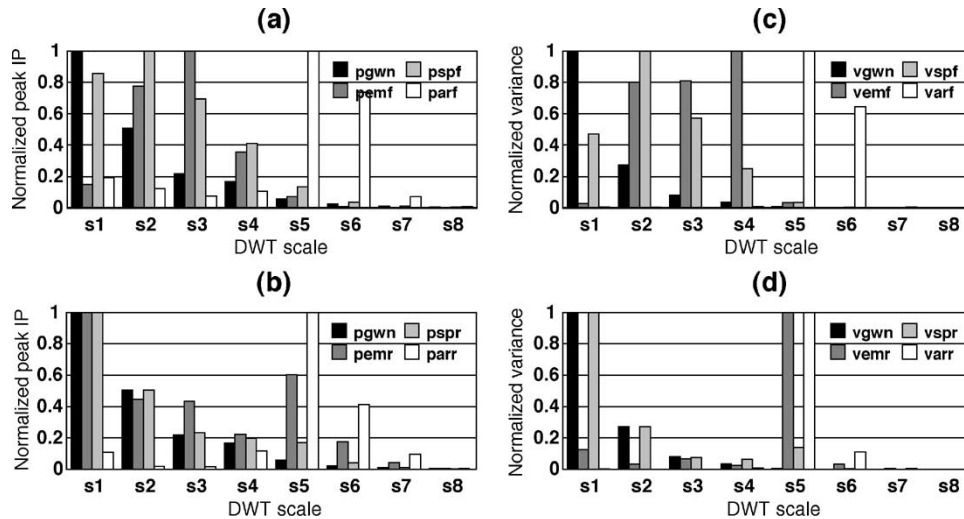


Fig. 2. (a) and (b) average normalized peak values ($pemf/pemr$, $pspf/pspr$, $parf/parr$) and (c) and (d) average normalized variances ($vemf/vemr$, $vspf/vspr$, $varf/varr$) of IP for each scale of forward–reverse flow components of ES, DS, and artifacts, respectively, as compared to GWN ($pgwn$, $vgwn$).

and narrower frequency bands. It is also obvious that there is an overlap between ES and DS. Therefore, it is impossible to differentiate an embolic event totally from normal DS. However, improvement in detecting ES is achievable by using the wavelet decomposition.

III. SUBJECTS AND METHOD

A. Data Collection for All Studies

The ES used for this study were recorded using a commercially available transcranial Doppler system (EME Pioneer TC4040) with a 2-MHz transducer. The recordings were made from the ipsilateral middle cerebral artery of 35 patients with symptomatic carotid stenosis. Recordings had been made onto digital audiotape. ES were identified subjectively by two experienced observers from both the FFT spectral display and the audio signal using conventional criteria [29]. The quadrature audio Doppler signals containing ES were exported to a personal computer for signal analysis. The sampling frequency was 7150 Hz. In order to evaluate the detection system, two independent data sets, each comprising 100 low intensity ES, 100 various type of artifacts and 100 DS were used. The total 200 artifacts were created artificially during patient recordings by tapping the probe (37), or by speech or coughing (66), or obtained from natural artifacts occurring during patient movement, speech, or coughing during routine patient recordings (93). After applying the DWT to the data, several parameters were evaluated. The threshold values used in both data sets were optimized using the first data set. An eighth-order Daubechies wavelet filter [27] was used for both data sets. The order of the filter were experimentally determined to be suitable for ES detection. The number of scales was eight. Only one cardiac cycle (approximately 1 s) was considered for the first data set. For the second data set, a standard 5-s duration segment including several cardiac cycles was considered. The second data set was developed to validate the detection algorithm which was devised from the first data set. The algorithm was also tested on a third data set

comprising 100 ES, which were recorded preoperatively from patients presented with 50% or more symptomatic internal carotid artery stenosis, and 102 ES, which were recorded from the patients underwent carotid endarterectomy. Only extracts of 5 s of each signal in this data set were used.

B. Detection Algorithm

A general block diagram of the detection system is shown in Fig. 3. The first step is to convert quadrature Doppler signals to the directional ones [30], [31]. This step is important to utilize one of the most distinctive features of ES. Most ES are unidirectional and most artifacts are bidirectional. Inputs of this block are N points in-phase signal $s_i(k)$ and quadrature signal $s_q(k)$. The outputs are forward signal $s_f(k)$ and reverse signal $s_r(k)$.

At the second stage, the DWT coefficients of the forward and reverse signals are obtained using an appropriate wavelet and number of scales. This process decomposes the input signal into an optimum number of frequency bands. Therefore, it is important to determine a suitable wavelet for the signal being analyzed. Suitability of the wavelet filters and orders were determined experimentally. From the experimental results, it was found that almost all ES are represented at the first four scales and artifacts were at the higher scales. This inherent feature of the DWT greatly simplifies artifact removal procedure by the scale domain filtering. The remaining individual scales are reconstructed by the IDWT using the same wavelet, and corresponding IP are calculated. A threshold level for each scale is determined. An example of a directional ES corrupted by a large artifact and corresponding reconstructed wavelet coefficients for five scales are shown in Fig. 4. Fig. 5 illustrates the associated normalized IP, which is used in the detection algorithm. An ES around the absolute time 400 ms is embedded in a very large artifact in the original forward Doppler signal. After the DWT, the ES is enhanced at the Scale 2. The noise appears at the Scale 1. DS appear at the Scales 2 and 3. Large artifact dominates Scales 4 and 5. Note that the ES is unidirectional, and the artifact is bidirectional, as the ratio of forward and reverse signal powers at this scale are approximately one.

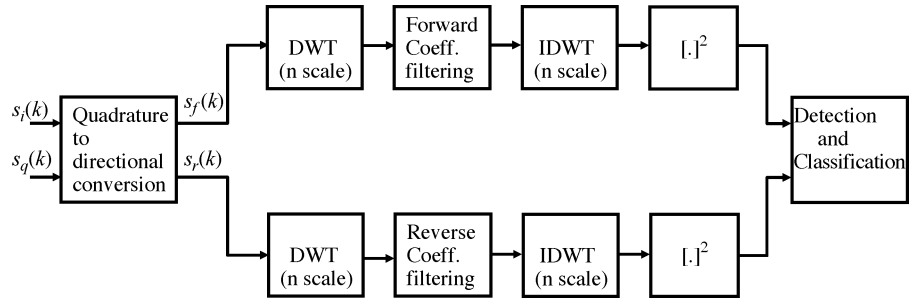


Fig. 3. Block diagram of the DWT-based detection system.

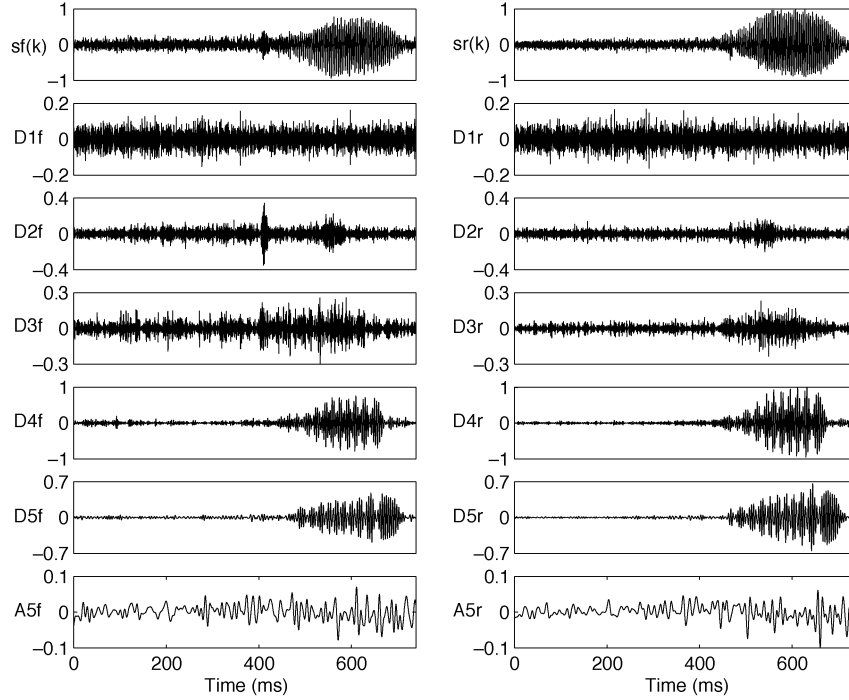


Fig. 4. Forward and reverse flow components of an ES corrupted with an artifact and corresponding reconstructed wavelet coefficients for five scales (f:forward, r:reverse).

At the final stage, detection and classification are performed. First, the scale, which is likely to contain the ES, is determined by using two parameters; the scale with maximum power (MP) and the scale with maximum peak to threshold ratio ($P2TR$), which is a definition of the EBR . If these two parameters refer to the same scale, then the classification is done on this scale. If these parameters refer to different scales, then the scale with maximum $P2TR$ is considered. This approach eliminated most of the mis-selection of the scales for further analysis and classification process. Additionally, existence of some components of the ES within a certain time margin in the neighboring scales are also investigated using the same criteria as above. If this is the case, then those scales are also considered for the detection.

Finally, for automatic detection, a decision system based on fuzzy logic rule was used [32]. The membership values for the most parameters were calculated according to the rules given in Table I, which were derived from the membership function illustrated in Fig. 6. Several thresholds were used to construct trapezoidal membership functions. The threshold values (th_1 , th_2 , th_3 , and th_4), which are given in Table II, were determined by statistical evaluation of the parameters used in the detection

such as calculation of minimum, maximum, mean, and standard deviation (Table III). The final decision if a signal is ES, DS, or artifact is based on average membership values of all the parameters for each signal types.

C. Parameters Used for the Detection and Classification of ES

One of the most important steps is the threshold selection. Because it is used as a normalizing factor in almost all parameters, the results are greatly influenced by the threshold. The threshold is determined from the data, which is sufficiently long, by using a statistical procedure, which depends on the data length and the standard deviation [33], and it is given by

$$A_{th} = \sigma_{fn} \sqrt{\log_2 N} + \sigma_{rn} \sqrt{\log_2 N} \quad (4)$$

where σ_{fn} and σ_{rn} are the standard deviations of the forward and the reverse signal power at the n th scale, and N is the length of the observation. The following parameters involving the threshold are determined.

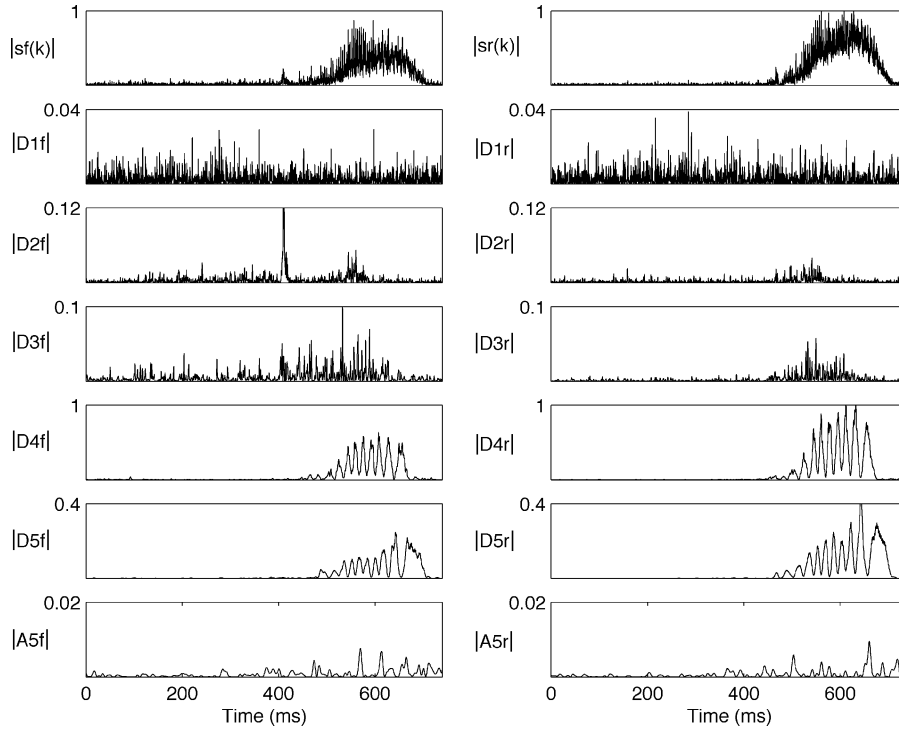


Fig. 5. Instantaneous envelopes of the reconstructed wavelet coefficients of the forward and reverse flow signals given in Fig. 4.

TABLE I
MEMBERSHIP RULES FOR THE PARAMETERS

$x(n)$	$< th_1$			$\geq th_1 \text{ \& \< } th_2$			$> th_2 \text{ \& \< } th_3$			$\geq th_3 \text{ \& \< } th_4$			$> th_4$		
	ar	em	sp	ar	em	sp	ar	em	sp	ar	em	sp	ar	em	sp
$P2TR$	0	0	1	0	z_1	$1 - z_1$	0	1	0	z_2	$1 - z_2$	0	1	0	0
$TP2TR$	0	0	1	0	z_1	$1 - z_1$	0	1	0	z_2	$1 - z_2$	0	1	0	0
$F2RM$	1	0	0	$1 - z_1$	0	z_1	0	0	1	0	z_2	$1 - z_2$	0	1	0
$TF2R$	1	0	0	$1 - z_1$	0	z_1	0	0	1	0	z_2	$1 - z_2$	0	1	0
RR	1	0	0	$1 - z_1$	z_1	0	0	1	0	0	$1 - z_2$	z_2	0	0	1
FR	1	0	0	$1 - z_1$	z_1	0	0	1	0	0	$1 - z_2$	z_2	0	0	1
t_s	0	0	1	0	$1 - z_1$	z_1	0	1	0	z_2	$1 - z_2$	0	1	0	0
f_s	0	0	1	0	z_1	$1 - z_1$	0	1	0	z_2	$1 - z_2$	0	1	0	0
T_s^2	0	0	1	0	$1 - z_1$	z_1	0	1	0	z_2	$1 - z_2$	0	1	0	0
B_s^2	1	0	0	$1 - z_1$	z_1	0	0	1	0	0	$1 - z_2$	z_2	0	0	1
VIE	0	0	1	z_1	0	$1 - z_1$	1	0	0	$1 - z_2$	z_2	0	0	1	0
VIF	1	0	0	$1 - z_1$	z_1	0	0	1	0	0	$1 - z_2$	z_2	0	0	1

ar: artifact, em: emboli, sp: speckle; $z_1 = (th_2 - th_1)^{-1}(x(n) - th_1)$, $z_2 = (th_4 - th_3)^{-1}(x(n) - th_3)$

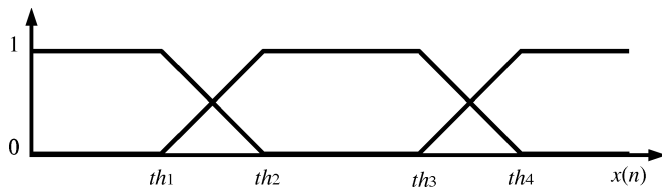


Fig. 6. Membership function for the derivation of membership values used in the automatic detection.

The most widely used parameter in ES detection is the EBR—indicating how strong an ES is relative to the background DS. One of the definitions of the EBR is the P2TR which can be calculated using the quantities given in Fig. 7

$$P2TR = 10 \log \frac{A_{pk}}{A_{th}} \quad (\text{dB}). \quad (5)$$

Another parameter, which indicates the amount of power a signal has relative to the background energy, is the total power to the threshold ratio (TP2TR) and given as

$$TP2TR = 10 \log \frac{A_{tot}}{A_{th}} = 10 \log \frac{\sum_{k=t_{on}}^{t_{off}} A_f(k)}{A_{th}} \quad (\text{dB}) \quad (6)$$

where A_{tot} is the total power of the ES. It is calculated by integrating the IP of forward signal ($A_f(k)$) between t_{on} and t_{off} , as shown in Fig. 7.

Two other parameters, which use threshold indirectly, are ES rise rate (RR) and fall rate (FR). They are defined as

$$RR = \frac{10 \log \frac{A_{pk}}{A_{th}}}{t_{pk} - t_{on}} = \frac{P2TR}{t_{pk} - t_{on}} \quad (\text{dB/ms}) \quad (7)$$

$$FR = \frac{10 \log \frac{A_{pk}}{A_{th}}}{t_{off} - t_{pk}} = \frac{P2TR}{t_{off} - t_{pk}} \quad (\text{dB/ms}). \quad (8)$$

TABLE II
 THRESHOLD VALUES OF THE PARAMETERS USED IN THE DETECTION

	th_1	th_2	th_3	th_4
$P2TR$ (dB)	6	12	14	20
$TP2TR$ (dB)	17	23	26	38
$F2RM$ (dB)	10	20	22	26
$TF2R$ (dB)	4	8	10	20
RR (ms)	0.6	1.4	2	5
FR (ms)	0.6	1.4	2	6
t_s (ms)	10	20	60	120
f_s/F_s (unit)	0.01	0.035	0.08	0.1
T_s^2 (ms ²)	6	18	40	100
B_s^2/F_s (unit)	0.03	0.06	0.1	0.4
VIE (unit)	12	60	100	140
VIF/F_s (unit)	0.008	0.016	0.021	0.04

$F_s = \text{Sampling frequency}$

 TABLE III
 MEAN AND STANDARD DEVIATIONS OF SOME PARAMETERS FOR EMBOLIC SIGNALS, ARTIFACTS, AND DS

	ES		Artifact		DS	
	Mean	SD	Mean	SD	Mean	SD
SMP	2.45	0.83	5.96	0.77	3.27	0.72
$TP2TR$	25.13	3.17	34.57	6.62	18.32	3.13
$P2TR$	12.1	3.01	14.16	6.67	6.29	1.82
$F2RM$	25.44	7.01	9.4	11.15	23.18	7.59
$F2R8$	1.29	7.13	1.79	11.25	-0.58	6.18
RR	3.88	2.53	0.95	0.59	3.52	2.05
FR	4.65	3.15	0.97	0.63	4.00	2.12
$TF2R$	15.30	6.24	4.05	9.82	14.13	4.03
t_s	51.59	31.7	146.38	76.8	6.96	4.9
f_s	0.114	0.049	0.014	0.007	0.108	0.189
T_s^2	73.87	43.3	185.08	106.6	10.86	8.6
B_s^2	0.08	0.038	0.033	0.031	0.492	0.438
VIE	101.34	96.1	43.47	63.3	12.3	5.6
VIF	0.016	0.008	0.012	0.021	0.021	0.012

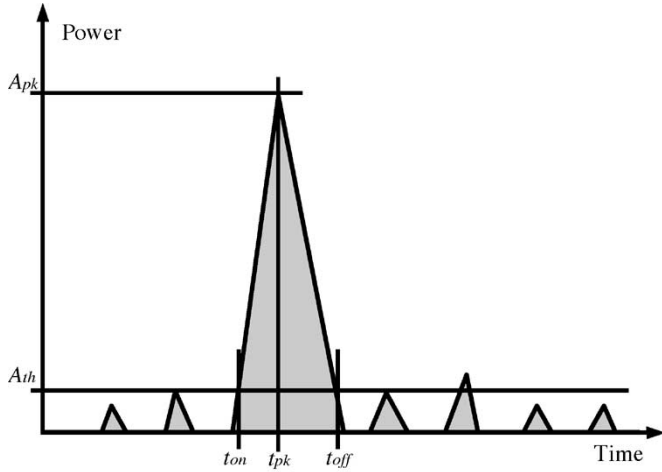


Fig. 7. Sketch of a specific reconstructed wavelet scale containing an ES and quantities used to calculate detection parameters.

Two parameters which utilize the directionality properties of ES are the peak forward to reverse power ratio at the scale ($F2RM$) and the total forward to reverse power ratio ($TF2R$) calculated over the duration between t_{on} and t_{off} . They are given as

$$F2RM = 10 \log \frac{A_f(t_{pk})}{A_r(t_{pk})} \quad (\text{dB}) \quad (9)$$

$$TF2R = 10 \log \frac{\sum_{k=t_{on}}^{t_{off}} A_f(k)}{\sum_{k=t_{on}}^{t_{off}} A_r(k)} \quad (\text{dB}) \quad (10)$$

where $A_f(k)$ and $A_r(k)$ are IP of forward and reverse signals, respectively.

Although the DWT decomposes an ES into different frequency bands, the frequency characteristics of ES cannot be utilized properly because of the poor frequency resolution of the DWT at higher frequency bands. The following parameters attempt to overcome this problem by utilizing some basic definitions of TF characterization of narrow-band signals in the context of information theory. Although some of these definitions are invalid for wide-band signals, the individual decomposed scales may be regarded as narrow-band signals. A simple way to characterize a signal simultaneously in time and frequency is to consider its mean localization and dispersions in each of these representations. This can be obtained by considering $|s(t)|^2$ and $|S(f)|^2$ as probability distributions, and looking at their mean values and standard deviations. t_s is the average time of the signal and f_s is the average frequency of the signal and are defined, respectively, as

$$t_s = \frac{1}{E_s} \int_{-\infty}^{+\infty} t |s(t)|^2 dt, \quad f_s = \frac{1}{E_s} \int_{-\infty}^{+\infty} f |S(f)|^2 df \quad (11)$$

where $S(f)$ is the Fourier transform of $s(t)$ and calculated by using the FFT. Time spreading (T_s^2) and frequency spreading (B_s^2) are defined as

$$T_s^2 = \frac{1}{E_s} \int_{-\infty}^{+\infty} (t - t_s)^2 |s(t)|^2 dt \quad (12)$$

$$B_s^2 = \frac{1}{E_s} \int_{-\infty}^{+\infty} (f - f_s)^2 |S(f)|^2 df \quad (13)$$

where

$$E_s = \int_{-\infty}^{+\infty} |s(t)|^2 dt < +\infty \quad (14)$$

A narrow-band signal then can be characterized in the TF plane by its mean position and a domain of main energy localization whose area is proportional to the time-bandwidth product.

Another way to describe a signal simultaneously in time and in frequency is to consider its instantaneous envelope and instantaneous frequency [28], which are defined, respectively, as

$$a(t) = |s_a(t)|, \quad f(t) = \frac{1}{2\pi} \frac{d \arg s_a(t)}{dt} \quad (15)$$

where $s_a(t) = s(t) + j\hat{s}(t)$, $\hat{s}(t)$ is the Hilbert transform of $s(t)$. In detection, algorithm variances of instantaneous envelope and instantaneous frequency (VIE , VIF) were used.

Processing steps for the detection of ES can be summarized as follows:

- 1) obtain directional Doppler signals by applying phasing filter technique to quadrature Doppler signals [30];
- 2) apply eight scales DWT to each channel in order to obtain directional DWT coefficients;
- 3) reconstruct individual wavelet coefficients;
- 4) calculate IP for each scales;
- 5) derive a threshold value from the signal for each scale to be used in detection;

- 6) evaluate previously described parameters for each scale;
- 7) apply detection logic.

IV. RESULTS

Mean values and standard deviations of the various signal characteristics for ES, DS, and artifacts are shown in Table III. The mean scale with maximum power (*SMP*) for ES and associated standard deviation (mean:2.45, standard deviation:0.83) implies that ES mainly appear at lower scales (dominantly at the Scales 2 and 3). However it must be pointed out that this will be affected by the system sampling frequency and choice of the analyzing wavelet. Therefore the candidate scales containing possible ES for further analysis are determined by identifying the scale with *MP* and *P2TR*. 13 out of 100 ES in the first data set had maximum intensity at the scale 1. 9 ES had maximum intensity at the scale 4. Some of these ES had some components at lower or higher scales because of the chirping characteristic. The mean *SMP* for artifacts (5.96, 0.77) shows that they appear at the higher scales (centered at the scale 6). The mean *SMP* for DS (3.27, 0.72) demonstrates that DS, which might be detected as ES, occupy mainly scale 3 spanning from the scale 2 to the scale 4. Although they were significantly different from ES ($P < 0.0001$), there is a certain overlap between the *SMP* for ES and DS. One practical conclusion, which can be derived from the *SMP* values, is that restricting the DWT analysis to the first 4 scales can eliminate most of the artifacts.

The average *TP2TR* for ES (25.13, 3.17 dB) is greater than the average *TP2TR* for DS (18.32, 3.13 dB) and less than the average *TP2TR* for artifacts (34.57, 6.62 dB). The average *P2TR* value for ES (12.1, 3.01 dB) is greater than the average *P2TR* value for DS (6.29, 1.82 dB) and less than artifacts (14.16, 6.77 dB). The average *F2RM* value reveals the directionality of a signal with maximum power at a certain scale and time. The average values for ES (25.44, 7.01 dB) and DS (23.18, 7.59 dB) suggest that they are unidirectional when compared to the average value of the *F2RM* for artifacts (9.4, 11.15 dB). This parameter is directly influenced by the ability of directional signal separation of the Doppler system used for the recordings. The average *F2R8* values [(1.29, 7.13 dB) for ES, (1.79, 11.25 dB) for artifacts, and (-0.58, 6.18 dB) for DS] suggest that there is no useful information at higher scales. These scales are mainly dominated by bidirectional slowly varying signals resulting from artifacts. ES result from an object passing through an ultrasonic sample volume causing a gradual intensity increase and then gradual decrease with a chirping effect when compared to artifacts. The average *RR* and *FR* for ES are (3.88, 2.53 ms) and (4.65, 3.15 ms), respectively. DS gave almost the same figures as ES [(3.52, 2.05 ms) and (4, 2.12 ms), respectively], suggesting that emboli and normal red blood cells have certain behavioral similarities. This can only be justified when both a red blood cell and an embolus are considered as a single scatterer. In practice, the size of the red blood cell is extremely small and beyond the detection resolution of any Doppler ultrasonic system. Instead red blood cell aggregates are scatterers producing a wide-band signal when compared to a signal resulting from an embolus, which is much bigger than that of red blood cells. Therefore,

TABLE IV
DETECTION RESULTS FOR TWO DATA SETS

Data set 1	Data set 2
100 ES	100 ES
98% as embolic signal	95% as ES
1% as artifact	3% as artifact
1% disputed	2% disputed
100 artifacts	100 artifacts
96% detected as artifact	98% as artifact
4% disputed	2% as ES
100 DS	100 DS
93% as DS	95% as DS
6% as ES	1% as artifact
1% disputed	4% disputed

the frequency band of an ES is much narrower, which validates the assumption of an embolus as a single scatterer.

The results obtained for two data sets are given in Table IV. It should be emphasized that these results may be influenced by the choice of the threshold values for certain parameters. ES are at least 3 dB greater than the DS. However, intercenter agreement greatly improves when the EBR is greater than 7 dB [34]. When the algorithm was tested on the third data set comprising ES mostly with the EBR ratio greater than 7 dB, 198 ES out of 202 were detected as ES.

V. DISCUSSION

Earlier ES detection systems assumed that the signal was stationary within the analysis window. However, ES are short duration nonstationary signals. The WT is a relatively new tool to deal with such signals. Our results suggest that the WT is likely to increase system sensitivity and specificity. The availability of fast algorithms and its ability to remove unwanted signals such as artifacts also make the WT attractive in on-line systems.

Artifacts propagate through more than three scales, suggesting that they are real transients in technical terms. At this point, the description of ES as transients is questionable. A transient is an unexpected complex signal disturbance having a range of frequency components. It can be considered as a wide-band signal compared to ES. ES can also be expressed within the context of wavelet theory. In fact, they are composed of several "wavelets" resulting from a single scatterer passing through an ultrasonic sample volume. They satisfy the basic properties of wavelets: ES oscillate and decay rapidly as wavelets do. Therefore, they were described as "frequency focused" as well as "short duration" high intensity transients.

In this study, we have used a signal-processing algorithm based on the DWT to characterize ES, DS, and artifacts. Results show that the detection parameters derived from the DWT coefficients are likely to improve the sensitivity of an automated system. In an automated ES detection system, there are several important aspects. First, the algorithm must emphasize ES and preferably suppress DS and artifacts. Such a feature will lead to an improvement in the EBR. This problem can be considered as the detection and estimation of signals in noise. The WT has been proved to be an effective tool for the detection and estimation of transients [35]. The statistical properties of the DWT for white noise and Doppler signals presented above enables us to accurately estimate a signal from a small number of

wavelet coefficients. ES are most likely to appear in the scales with larger variance. If there is an unusual activity within the analysis window, this will be reflected on the variance. This is true because the energy of an ES born by a potentially symptomatic embolus is much greater than the energy of the signal from DS. A practical conclusion from this observation is that a simple WT process can be employed to enhance any Doppler signal or an ultrasonic image by simply canceling out related wavelet coefficients during reconstruction. However, one drawback of the DWT compared to the FFT is the reduced frequency resolution at lower scales, in which ES are found mostly. The performance of the DWT-based system alone may not be as good as an FFT-based system due to the lack of frequency resolution although it does have some advantages for very small signals due to its high temporal resolution. Therefore, we have introduced some additional parameters based on the FFT and instantaneous frequency to be used in the detection algorithm.

Our system was evaluated on 5-s segments of data, each containing an ES artifact or DS, and processed in real time. This is the most efficient method to develop a system which analyzes signals which may occur rarely. For example only 40% of patients with symptomatic carotid stenosis, and 5%–10% of patients with asymptomatic stenosis have ES during an hours recording, and in those patients who have ES, the median number is only one or two. Our wavelet-based approach now needs to be implemented in a true on-line system which can operate in real time. The performance of this system could then be directly compared with other on-line systems using different approaches such as the frequency filtering approach using the FFT [36]. This is feasible as the DWT is a computationally efficient transform.

REFERENCES

- [1] M. P. Spencer, G. I. Thomas, S. C. Nicholls, and L. R. Sauvage, "Detection of middle cerebral artery emboli during carotid endarterectomy using transcranial Doppler ultrasonography," *Stroke*, vol. 21, pp. 415–423, 1990.
- [2] H. S. Markus and M. J. Harrison, "Microembolic signal detection using ultrasound," *Stroke*, vol. 26, pp. 1517–1519, 1995.
- [3] H. S. Markus, R. Ackerstaff, V. Babikian, C. Bladin, D. Droste, D. Grossett, C. Levi, D. Russell, M. Siebler, and C. Tegeler, "Inter-centre agreement in reading Doppler embolic signals: a multicentre international study," *Stroke*, vol. 28, pp. 1307–1310, 1997.
- [4] R. G. A. Ackerstaff, V. L. Babikian, D. Georgiadis, D. Russell, M. Siebler, M. P. Spencer, and D. Stump, "Basic identification criteria of Doppler microembolic signals," *Stroke*, vol. 26, p. 1123, 1995.
- [5] E. Roy, P. Abraham, S. Montrésor, M. Baudry, and J. L. Saumet, "The narrow band hypothesis: an interesting approach for high-intensity signals (HITS) detection," *Ultrasound Med. Biol.*, vol. 24, pp. 375–382, 1998.
- [6] H. S. Markus, A. Loh, and M. M. Brown, "Computerized detection of cerebral emboli and discrimination from artifact using Doppler ultrasound," *Stroke*, vol. 24, pp. 1667–1672, 1993.
- [7] M. P. Spencer, "Detection of cerebral arterial emboli," in *Transcranial Doppler*, D. W. Newell and R. Aaslid, Eds. New York: Raven Press, 1995, pp. 215–230.
- [8] E. V. Van Zuijlen, W. H. Mess, C. Jansen, I. Van der Tweel, J. van Gijn, and R. G. A. Ackerstaff, "Automatic embolus detection compared with human experts: a Doppler ultrasound study," *Stroke*, vol. 27, pp. 1840–1843, 1996.
- [9] B. Brucher and D. Russell, "Spectral characteristics of emboli with artifact suppression," *Stroke*, vol. 24, p. 510, 1993.
- [10] M. Siebler, G. Rose, M. Sitzer, A. Bender, and H. Steinmetz, "Real-time identification of cerebral microemboli with US feature detection by a neural network," *Radiology*, vol. 192, pp. 739–742, 1994.
- [11] D. Georgiadis, J. Goeke, M. Hill, M. Konig, D. G. Nabavi, F. Stögbauer, P. Zunker, and E. B. Ringelstein, "A novel technique for identification of Doppler microembolic signals based on the coincidence method—in vitro and in vivo evaluation," *Stroke*, vol. 27, pp. 683–686, 1996.
- [12] E. Roy, S. Montrésor, P. Abraham, and J. L. Saumet, "Spectrogram analysis of arterial Doppler signals for off-line automated HITS detection," *Ultrasound Med. Biol.*, vol. 25, pp. 349–359, 1999.
- [13] E. Roy, P. Abraham, S. Montrésor, and J. L. Saumet, "Comparison of time-frequency estimators for peripheral embolus detection," *Ultrasound Med. Biol.*, vol. 26, pp. 419–423, 2000.
- [14] H. Markus and G. Reid, "Improved automated detection of embolic signals using a novel frequency filtering approach," *Ultrasound Med. Biol.*, vol. 25, pp. 857–860, 1999.
- [15] L. Fan, D. H. Evans, and A. R. Naylor, "Automated embolus identification using a rule-based expert system," *Ultrasound Med. Biol.*, vol. 27, pp. 1065–1077, 2001.
- [16] W. H. Mess, B. M. Titulaer, and R. G. A. Ackerstaff, "A new algorithm for off-line automated emboli detection based on the pseudo-Wigner power distribution and dual gate TCD technique," *Ultrasound Med. Biol.*, vol. 26, pp. 413–418, 2000.
- [17] G. Devuyt, J.-M. Vesin, P.-A. Despland, and J. Bogousslavsky, "The matching pursuit: A new method of characterizing microembolic signals?," *Ultrasound Med. Biol.*, vol. 6, pp. 1051–1056, 2000.
- [18] G. Devuyt, G. A. Darbellay, J.-M. Vesin, V. Kemény, M. Ritter, D. W. Droste, C. Molina, J. Serena, R. Sztajzel, P. Ruchat, C. Lucchesi, G. Dietler, E. B. Ringelstein, P.-A. Despland, and J. Bogousslavsky, "Automatic classification of HITS into artifact or solid or gaseous emboli by a wavelet representation combined with dual-gate TCD," *Stroke*, vol. 32, pp. 2803–2809, 2001.
- [19] M. A. Moehring and M. P. Spencer, "Power M-mode Doppler (PMD) for observing cerebral blood flow and tracking emboli," *Ultrasound Med. Biol.*, vol. 28, pp. 49–57, 2002.
- [20] N. Aydin, S. Padayachee, and H. S. Markus, "The use of the wavelet transform to describe embolic signals," *Ultrasound Med. Biol.*, vol. 25, pp. 953–958, 1999.
- [21] B. S. Krongold, A. M. Sayeed, M. A. Moehring, J. A. Ritcey, M. P. Spencer, and D. I. Jones, "Time-scale detection of microemboli in flowing blood with Doppler ultrasound," *IEEE Trans. Biomed. Eng.*, vol. 46, pp. 1081–1089, Sept. 1999.
- [22] J.-M. Girault, D. Kouame, A. Ouahabi, and F. Patat, "Micro-emboli detection: an ultrasound Doppler signal processing viewpoint," *IEEE Trans. Biomed. Eng.*, vol. 47, pp. 1431–1439, Nov. 2000.
- [23] N. Aydin, H. S. Markus, and F. Marvasti, "Detection and estimation of embolic Doppler signals using discrete wavelet transform," in *Proc. ICASSP 2001*, vol. 2, 2001, pp. 1049–1052.
- [24] S. Mallat, *A Wavelet Tour of Signal Processing*. San Diego, CA: Academic, 1998.
- [25] R. K. Young, *Wavelet Theory and its Applications*. Norwell, MA: Kluwer, 1993.
- [26] G. Strang and T. Nguyen, *Wavelets and Filter Banks*. Cambridge, MA: Wellesley-Cambridge, 1997.
- [27] I. Daubechies, *Ten Lectures on Wavelets*. Philadelphia, PA: SIAM, 1992, CBMS Lecture Series.
- [28] B. Boashash, "Estimating and interpreting the instantaneous frequency of a signal: a tutorial review—part 2: Algorithms and applications," *Proc. IEEE*, vol. 80, pp. 539–568, Apr. 1992.
- [29] E. B. Ringelstein, D. W. Droste, V. L. Babikian, D. H. Evans, D. G. Grosset, M. Kaps, H. S. Markus, D. Russell, and M. Siebler, "Consensus on microembolus detection by TCD," *Stroke*, vol. 29, pp. 725–729, 1998.
- [30] N. Aydin, L. Fan, and D. H. Evans, "Quadrature-to-directional format conversion of Doppler signals using digital methods," *Physiol. Meas.*, vol. 15, pp. 181–199, 1994.
- [31] N. Aydin and D. H. Evans, "Implementation of directional Doppler techniques using a digital signal processor," *Med. Biol. Eng. Comput.*, vol. 32, pp. S157–S164, 1994.
- [32] H. Seker and M. Korurek, "Fuzzy relation matrix and fuzzy max-min operation for biomedical signal classification," in *Proc. 2nd Int. Biomedical Engineering Days '98*, Istanbul, Turkey, May 1998, pp. 57–59.
- [33] D. L. Donoho, "De-noising by soft-thresholding," *IEEE Trans. Inform. Theory*, vol. 41, pp. 613–647, May 1995.
- [34] H. S. Markus, M. Bland, G. Rose, M. Sitzer, and M. Siebler, "How good is intercenter agreement in the identification of embolic signals in carotid artery disease?," *Stroke*, vol. 27, pp. 1249–1252, 1996.
- [35] J. P. Noonan, H. M. Polhlopek, and M. Varteresian, "A hypothesis testing technique for the wavelet transform in the presence of noise," *Digital Signal Process.*, vol. 4, pp. 89–96, 1993.

- [36] M. Cullinane, G. Reid, R. Dittrich, Z. Kaposzta, R. Ackerstaff, V. Babikian, D. W. Droste, D. Grossett, M. Siebler, L. Valton, and H. S. Markus, "Evaluation of a new on-line automated embolic signal detection algorithm, including comparison with a panel of international experts," *Stroke*, vol. 31, pp. 1335–1341, 2000.



Nizamettin Aydin (M'92) received the B.Sc. and MSc degrees in electronics and communication engineering from Yildiz Technical University, Istanbul, Turkey, in 1984 and 1987, respectively, and the Ph.D. degree in medical physics from the University of Leicester, Leicester, U.K., in 1994.

Between 1986 and 1989, he worked as a Research and Teaching Associate in the Electrical Engineering Department, Yildiz Technical University. He was an Associate Professor in the Electronic Engineering Department, Gebze Institute of Technology, Turkey, from 1995 to 1999. He also worked in the Department of Clinical Neurosciences at King's College London and the Division of Clinical Neuroscience at St. George's Hospital Medical School as a Research Fellow between 1998 and 2001. He is currently a Senior Research Fellow in the School of Engineering and Electronics, University of Edinburgh, Edinburgh, U.K. His current research interests include time-frequency and time-scale analysis, physiological measurements with Doppler ultrasound, digital signal processing, VLSI, system-on-chip design, low-power digital design, and wireless communication.

Dr. Aydin was awarded the IEE Institute Premium Award for 2000/2001. He is an Associate Editor of the IEEE TRANSACTIONS ON INFORMATION TECHNOLOGY IN BIOMEDICINE.



Farokh Marvasti (S'72–M'74–SM'83) received the B.Sc., M.Sc., and Ph.D. degrees from Rensselaer Polytechnic Institute, Troy, NY, in 1970, 1971, and 1973, respectively.

He has worked, consulted, and taught in various industries and academic institutions since 1972, among which are Bell Laboratories, University of California Davis, Illinois Institute of Technology, University of London, King's College. He has about 50 journal publications and has written several reference books. His recent book is *Nonuniform Sampling: Theory and Practice* (Norwell, MA: Kluwer, 2001). He is currently a Professor at Sharif University of Technology, Tehran, Iran, and the Director of Multimedia Laboratories, Iran Telecommunications Research Center.

Dr. Marvasti was one of the Editors and Associate Editors of IEEE TRANSACTIONS ON COMMUNICATIONS AND SIGNAL PROCESSING from 1990 to 1997.



Hugh S. Markus received the B.A. degree from Cambridge University, U.K., in 1981, and the B.M. Bch. from Oxford University, U.K., in 1984. He received the D.M. degree from Oxford University, U.K., in 1994.

He trained in neurology and was initially Senior Lecturer and then Reader in Neurology at King's College, London. In 2000, he was appointed to a Foundation Chair of Neurology at St. George's Hospital Medical School, London, U.K. He has been working in the field of embolic signal detection since 1992,

initially validating the technique in models systems and later developing both its clinical applications and automated systems for embolic signal detection.